ϵ	= turbulent diffusion coefficient, sq. ft./hr.			

ϵ = turbulent diffusion coefficient, sq. ft./hr.
θ = time, hr.
μ = viscosity, lb.-mass/ft. hr.
ρ = density, lb.-mass/cu. ft.
ϕ = interaction term
Φ = functional symbol
ψ = interaction term

Subscripts

b = binary
e = equimolal transfer
f = across film
F = outer edge of film
i, j = species 1, 2, or 3
l, L, O = positions
m = log mean unless otherwise defined
n = species n
S = transfer with one gas stagnant
T = across turbulent core
σ = sum of $n-1$ similar species
$1,2,3$ = respective species
I = interface

— = vector if below quantity, mean or bulk value if above
∇ = del operator

LITERATURE CITED

1. Bird, R .B., W. E. Stewart, and E. N. Lightfoot, "Transport Phenomena," Wiley, New York (1960).
2. Chilton, T. H., and A. P. Colburn, Ind. Eng. Chem., **26**, 1183 (1934).
3. Colburn, A. P., and T. B. Drew, Trans. Am. Inst. Chem. Engrs., **33**, 197 (1937).
4. Duncan, J. B., Ph.D. thesis, Carnegie Institute of Technology, Pittsburgh, Pennsylvania (1960).
5. Fairbanks, D. F., and C. R. Wilke, Ind. Eng. Chem., **42**, 471 (1950).
6. Hoopes, J. W., Jr., Ph.D. thesis, Columbia University, New York, New York (1951).
7. Hougen, O. A., and K. M. Watson, "Chemical Process Principles," Part 3, Wiley, New York (1948).
8. Keyes, J. J., Jr., and R. L. Pigford, Chem. Eng. Sci., **6**, 215 (1957).
9. Lin, C. S., R. W. Moulton, and G. L. Putnam, Ind. Eng. Chem., **45**, 636 (1953).
10. Maxwell, J. C., "Scientific Papers," Vol. 2, Dover, New York (1952).
11. Mickley, H. S., R. C. Ross, A. L. Squyers, and W. E. Stewart, Natl. Advisory Comm. Aeronaut. Tech. Note 3208 (1954).
12. Prandtl, L., Physik Z., **11**, 1072 (1910).
13. Sherwood, T. K., "Absorption and Extraction," McGraw-Hill, New York (1937).
14. Taylor, G. I., Advisory Comm. Aeronaut. (Great Britain) Tech. Rept. 272 (1916).
15. Toor, H. L., A.I.Ch.E. Journal, **3**, 198 (1957).
16. ——, and J. M. Marchello, ibid., **4**, 97 (1958).
17. Toor, H. L., ibid., **6**, 525 (1960).
18. von Karman, Theodore, Trans. Am. Soc. Mech. Engrs., **61**, 705 (1939).
19. Wilke, C. R., Chem. Eng. Progr., **46**, 95 (1950).

II. Experiment

Measurements have been made of the simultaneous rates of transfer of acetone and benzene between a liquid film and a turbulent three component gas mixture. The measurements were made in a wetted-wall column with both mixtures of acetone, benzene and nitrogen, and acetone, benzene and helium.

As predicted by the equations of Part I the mass transfer differs qualitatively as well as quantitatively from mass transfer in the corresponding binary system in which one component is stagnant. In several experiments acetone was transferred from low to high concentrations in accord with the predictions.

Both the ternary film and Prandtl-Taylor models satisfactorily predict the rates of transfer of acetone and benzene, and, except possibly for very high Reynolds numbers, the simpler film model is recommended.

The ternary convective mass transfer theory developed in Part I is concisely summarized by

$$N_i = k_i\, \phi\, (\delta\, y_{iI} - \overline{y}_i) \qquad (1)$$

where i takes on the values 1 and 2 and k_i, ϕ, and δ are functions which are positive and depend upon the type of transfer (equimolal or one component stagnant) and upon the type of model used. It is the object of this work to determine experimentally whether or not ternary convective mass transfer is described by an equation of the above form and which, if any, of the models developed in Part I is most suitable.

CHOICE OF SYSTEM

The conditions required for a satisfactory test of the rate equations are most readily obtained by contacting a volatile binary liquid below its bubble point with a ternary gas in which two of the species are common to the liquid and one is insoluble in the liquid.

This choice of a binary liquid phase greatly enlarges the choice of systems for which vapor-liquid equilibrium data are available and reduces the uncertainties concerning the mass transfer in the liquid phase. Furthermore the insoluble gas, which will be stagnant, can be readily changed to change the predicted interactions.

The system benzene-acetone, for which good equilibrium data are available (1), was chosen for the liquid phase, and both nitrogen and helium were used separately as the stagnant gases. The former tends to give relatively weak interactions, $r = 2.5$, and the latter relatively strong interactions, $r = 10$. [Note that r enters Equation (12), Part I, as an exponent.] In addition the choice of heavy species for those being transferred and light species for the inerts makes D_{13} close to D_{23}, so Equation (68), Part I, should hold, affording a useful check on the consistency of the theory and experiment.

EQUIPMENT AND PROCEDURE

The apparatus is shown schematically in Figure 1. A wetted-wall column similar to that used by Emmert and Pigford (3) was used to contact the gas and liquid. Operation was concurrent downwards. The 0.985-in. I.D. Pyrex glass pipe was 24 in. long measured from the knife edge at the top to the beginning of the take off flare at the bottom. The column was preceded by an 18 in. calming section made of 1-in. diameter brass pipe.

Both the gas and liquid streams were passed through preheaters and then through copper tubes in a constant temperature water bath. The gas was supplied simultaneously from a battery of four cylinders connected by a manifold. The liquid was pumped from a 50-gal. storage tank. Both the gas line from the constant-temperature bath and the calming section were insulated, the column was uninsulated, and the gas line leaving the column was electrically heated.

Provision was made for splitting the gas stream and passing a metered portion of it through a saturater which could be filled with either of the volatile species. Mixing of the saturated side stream with the main gas stream took place in a vertical packed section of pipe located in the constant-temperature bath.

The liquid and gas flow rates were measured by rotameters, and column pressure was determined by pressure taps

located before and after the column. Inlet and exit temperatures were determined by thermometers. Inlet and outlet gas and liquid compositions were determined by withdrawing samples and analyzing them by gas chromatography. The exit gas passed through 18 in. of 1-in. brass pipe and 5 ft. of ½-in. copper tubing before the exit gas sample was withdrawn. The gas samples were collected in 250 cc. gas sampling tubes by mercury displacement. Access to the gas stream was obtained by inserting a hypodermic tube through a rubber seal. Liquid samples of approximately 100 cc. were drawn through taps in the liquid lines. Analysis of samples was carried out immediately to prevent loss or contamination. A gas chromatograph was used with a calibrated 2.5 m. column and hydrogen carrier gas. The amount of each species present in a sample could be determined with a precision equal to about 1.5% of the amount of the species present.

The mean flux over the column (defined as the rate of transfer over the entire column divided by the apparent interfacial area) was obtained for each species by a material balance on the gas phase. When it was possible, fluxes were also computed from the liquid measurements.

After passing through the system the liquid was cooled and pumped to a storage tank and the gas was discarded. The materials used had purities ranging from 99.5 to 99.99%.

At the start of a run the temperatures in the preheaters and in the constant-temperature bath were adjusted to the desired level, and the liquid phase was circulated through the apparatus until the contents of the liquid reservoirs of the wetted-wall column reached a steady temperature. The gas flow was then started. The gas stream was either sent to the column as a pure gas or was split into two streams, and the side stream was saturated with acetone before being remixed with the main stream. When all temperatures reached a steady value, liquid and gas samples were withdrawn. Downstream samples were taken first to avoid disturbing column operation.

APPLICATION OF THE THEORY

The rate equations which have been developed contain interfacial compositions, and these must be eliminated (or evaluated) before the equations can be applied to the column. The rate equations for the binary liquid phase may, for simplicity, be written in the form

$$N_i = k_{Li} (\overline{x_i} - x_{iI}) \qquad (2)$$

and the $k_L's$ are not necessarily equal nor constant.

If interfacial equilibrium exists

$$y_{iI} = m_i x_{iI} \qquad (3)$$

and by the usual definition

$$y_i^* = m_i \overline{x_i} \qquad (4)$$

From Equations (1) to (4)

$$N_i = K_i \phi (\delta y_i^* - \overline{y_i}) \qquad (5)$$

and

$$\frac{1}{K_i} = \frac{1}{k_i} + \frac{m_i \delta \phi}{k_{Li}} \qquad (6)$$

The functions ϕ and δ however still depend formally upon the y_{iI}.

It is noteworthy that the effect of gas side interactions carries over into the over-all equation, for the over-all driving force retains the form of a generalized driving force. It follows that phenomena, such as reverse diffusion, can take place in a system even when an interacting region is in series with a noninteracting one.

Equation (6) shows that the liquid side resistance is given by the group $m_i \delta \phi / k_{Li}$ rather than by the normal group m_i / k_{Li}. The liquid side resistance also enters into the functions ϕ and δ through its effect on the y_{iI}, but in the system under study this effect is very weak so the former group has the characteristics of a normal liquid resistance.

If the k_L obtained in binary rectification in a wetted-wall column with liquid-mixtures similar to the one studied here (5) are used in Equation (6), it is found that the effect of liquid resistance is small, for the $\delta \phi$ product is almost always less than 1 and the m_i are small.

However in this study the k_{Li} do not necessarily equal the k_L reported for rectification, for the k_{Li} must be a function of the ratio N_1/N_2 and the two liquid side coefficients are not equal; in fact one must be negative when N_1 and N_2 have the same sign. These variations in the k_{Li} are of course caused by the bulk motion which exists in the liquid when N_1 does not equal $-N_2$.

When the k_{Li} which are corrected for the effect of bulk motion are used in Equation (6), it is found that the liquid side resistance has less than a 10% effect on the fluxes over the column. These effects are insignificant in the present study, so in the following development liquid resistance will be assumed equal to zero. The experimental results also show no sign of a liquid resistance. Thus with a zero liquid resistance K_i equals k_i and y_{iI}, which appears in ϕ and δ, equals y_i^*.

The final interacting rate equations which are to be compared to experiment now are

$$N_i = k_i \phi (\delta y_i^* - \overline{y_i}) \qquad (7)$$

and the functions k_i, ϕ, and δ from Part I take on the following forms for the present system in which component 3 is stagnant:

film

$$\phi = \frac{\ln(y_3^*/\overline{y_3})}{(1 - \overline{y_3}) - \delta(1 - y_3^*)} \qquad (8)$$

$$\delta = (\overline{y_3}/y_3^*)^r \qquad (9)$$

$$k_i = \frac{f}{2} G_m \left(\frac{\mu}{\rho D_{i3}} \right)^{-2/3} \qquad (10)$$

Prandtl-Taylor

$$\phi = \frac{\ln \delta_T}{\delta_T - 1} \qquad (11)$$

$$\delta = (\overline{y_3}/y_3^*)^{1+s(r-1)} \qquad (12)$$

$$k_i = \frac{f}{2} G_m /$$

$$\left[\left(\frac{\mu}{\rho D_{i3} \psi} - 1 \right) y_F^+ \sqrt{\frac{f}{2}} + 1 \right] \qquad (13)$$

$$\delta_T = (\overline{y_3}/y_3^*)^{1-s} \qquad (14)$$

$$\psi = \frac{s}{1-s} \frac{(1 - \delta_T)}{(\delta_T - \overline{y_3}) - \delta(1 - y_3^*)} \qquad (15)$$

$$s = \frac{y_F^+ \sqrt{\frac{f}{2}} \left(\frac{\mu}{\rho D_m} \right)}{\left(\frac{\mu}{\rho D_m} - 1 \right) y_F^+ \sqrt{\frac{f}{2}} + 1} \qquad (16)$$

Chilton-Colburn

Same as Prandtl-Taylor except

$$k_i = \frac{f}{2} G_m \left(\frac{\mu}{\rho D_{i3} \psi} \right)^{-2/3} \qquad (17)$$

$$s = y_F^+ \sqrt{\frac{f}{2}} \left(\frac{\mu}{\rho D_m} \right)^{1/3} \qquad (18)$$

The ratio u_F/V which appeared in the earlier Prandtl-Taylor form of the equations has been replaced, as usual, by $y_F^+ \sqrt{f/2}$, and y_F^+ will be taken as 11.6 which corresponds to the intersection of the laminar and turbulent velocity profiles. Equation (10), which is essentially a definition of the binary coefficient, is written in this form since it satisfactorily correlates a wide variety of earlier binary data (9), and while it is not the best fit, it is close to the results obtained in the preliminary binary runs made here.

If species j is dilute, then species i is not affected by species j and species i should behave as if it were in a binary mixture of itself with species 3. As expected Equation (7) reduces under these conditions to the normal binary equation when the film and Prandtl-Taylor models are used:

$$N_i = k_i \frac{(y_i^* - \overline{y_i})}{(y_3)_m} \qquad (19)$$

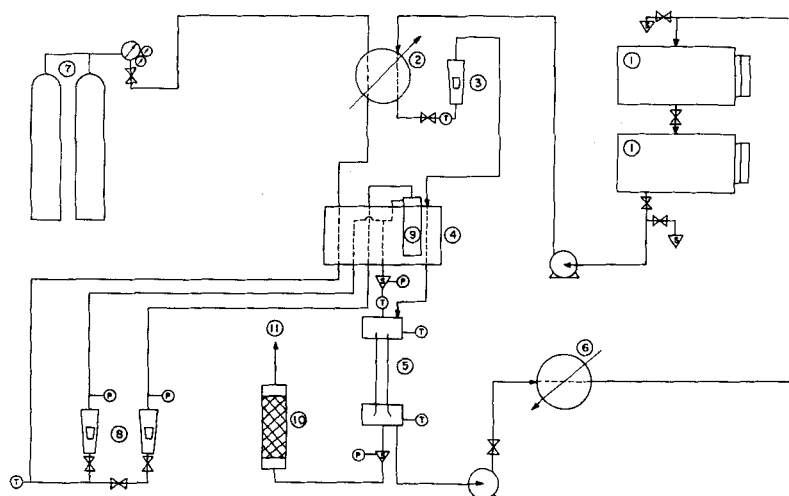where k_i is given by Equation (10) or (13). If both species 1 and 2 are di-

Fig. 1. Schematic diagram of equipment.

- ① LIQUID STORAGE AND SUPPLY
- ② PREHEATER
- ③ LIQUID ROTAMETER
- ④ CONSTANT TEMPERATURE BATH
- ⑤ WETTED WALL COLUMN
- ⑥ COOLER
- ⑦ GAS CYLINDERS AND MANIFOLD
- ⑧ PARALLEL GAS ROTAMETERS
- ⑨ GAS SATURATOR
- ⑩ WASTE GAS WASHER
- ⑪ VENT
- Ⓣ THERMOMETERS
- Ⓟ PRESSURE TAPS
- Ⓥ SAMPLING TAPS

lute, Equation (19) applies to both species and neither of the diffusing species interacts with the other; both behave as if they were in a binary mixture. [Although there is some question about the form of the $(y_3)_m$ term in Equation (19), the difference between this form and the other suggested forms (2, 10, 16) is not great enough to seriously affect this work.]

Clearly any test of Equation (7) is trivial unless the interactions are large enough to make the fluxes predicted by this equation differ significantly from the fluxes predicted by Equation (19), the noninteracting equation. It is the differences between these two equations which are of interest, for the question to be answered by experiment is whether or not the predicted interactions really occur.

Consequently the procedure to be followed here is to compare the predictions of both the interacting and noninteracting equations with experiment. Equation (10) will be used for the k_i in Equation (19). Since Equation (19) also describes the equivalent binary system discussed in Part I, this procedure also aids in understanding the behavior of the ternary system.

The convective mass transfer equations based on effective diffusivities and film thicknesses which were discussed in Part I were not used, since in many of the runs the effective diffusivity of one of the species is negative and the mass transfer coefficient is undefined. Although it was pointed out that these equations could be modified to eliminate this difficulty, these modified equations were not used since they are in essence the same as the present film model equations.

Similarly use of the exact film solution to the Maxwell-Stefan equations in place of the approximate equations

which were used is a refinement hardly warranted at present. (Trial calculations indicate that in the present study the errors caused by the use of the approximate equations in place of the exact equations are probably insignificant.)

It was shown in Part I that if $D_{13} = D_{23}$, then it must be true (independently of the present interaction theories) that the total flux follows the normal binary equation. With negligible liquid resistance

$$[N_1 + N_2]_{D_{13}=D_{23}} = k_b' \frac{\overline{y_3 - y_3^*}}{(y_3)_m} \quad (20)$$

and k_b' is given by Equation (10).

The interacting equations based on the film and Prandtl-Taylor models satisfy this criterion [strictly speaking k_b' should be given by Equation (29), Part I, for the Prandtl-Taylor model] and so do the noninteracting Equations (19), but the equations based on the Chilton-Colburn approach do not. In this work D_{13} is close to D_{23}, so Equation (20) would be expected to be a good approximation for the self-consistent models.

Although the total flux $N_1 + N_2$ predicted by the interacting and noninteracting equations should be about the same, except possibly for the inconsistent modified Chilton-Colburn model, the individual fluxes predicted by the interacting equations can be radically different from those predicted by the noninteracting equations. A severe test of the interacting equations can be attained for example by determining whether the reverse transfer which they predict does occur.

CALCULATION METHODS

In previous work on binary system investigators have assumed that mass

transfer coefficients could be computed from logarithmic mean driving forces based on terminal compositions (4). This method of averaging is quite successful for binary systems and was used here in the preliminary binary runs; however it cannot be applied to multicomponent systems, for both the ordinary binary driving forces and the generalized multicomponent driving forces can change sign in a column. (It can be used for the total flux, as will be seen.) For this reason it is necessary to postulate a mass transfer equation; combine the rate equations with a material balance, heat balance, and equilibrium data; and then numerically integrate down the column. The calculated exit compositions or mean fluxes can then be compared with the measured values as a test of the validity of the rate equations used.

In order to carry out the calculations the interfacial temperature must be known. A precise estimation is difficult, but heat transfer considerations indicate that the interfacial temperature is not likely to differ greatly from the bulk temperature. (There will be further discussion of this important point later.) Since the mean total flux was always positive, that is a net vaporization took place, the bulk liquid temperature decreased down the column. An accurate calculation of this temperature at every point in the column was not feasible and fortunately was unessential since the calculations were found to be relatively insensitive to liquid temperature.

Two different methods of calculating the bulk liquid temperature were used. In heat balance method a all of the net heat of vaporization was assumed to be supplied by the liquid phase. This method usually yields a calculated

value for the exit liquid temperature lower than the measured value.

In method *b* the heat balance was adjusted so that the computed exit temperature equaled, on the average, the measured exit temperature when the computed mean total flux was equal to the experimental value. Since it was found experimentally that on the average the liquid temperature change over the column corresponded to 70% of the total latent heat which had to be supplied, the adjustment was carried out by assuming that for each increment the liquid supplied only 70% of the net latent heat of vaporization required at that increment.

In most of the nitrogen runs the mean total flux was small, and the corresponding temperature drops were also small. In these runs (T1 to T5 inclusive) only method *a* was applied since the adjustment involved in method *b* was small.

In difference form Equation (7) becomes

$$N_i \, \Delta A = k_i \, \phi \, (\delta y_i{}^* - \overline{y}_i) \Delta A = \Delta n_i$$
(21)

and with measured inlet compositions, temperatures, and flow rates numerical integration was carried out on an IBM-650 digital computer. Because of the parallel flow of gas and liquid the calculations are straightforward. Twenty four increments were found to give sufficient accuracy. Compositions, flow rates, and liquid temperature were obtained at each increment for each of the rate equations under consideration: the ternary film, Prandtl-Taylor and modified Chilton-Colburn equations, Equations (7) to (18), and the noninteracting Equation (19).

Variations in physical properties and flow rates down the column were taken into account, but the bulk gas temperature was assumed to remain constant since the small changes in gas temperature have little effect on the rate equations. The Koo equation (6) was used for the friction factor, and the gas velocity with respect to the wall was used. The binary diffusion coefficients were calculated by the method of Hirschfelder, et al. (7) at an average gas film temperature. The Lennard-Jones force constants for nitrogen, helium, and benzene obtained from viscosity data and listed in the above reference were used, and those for acetone were estimated from the recommended reduced correlations. Typical values of the diffusion coefficients are shown in Table 1. The vapor-liquid equilibrium data of Canjar and Lonergan (1) was used to obtain $y_i{}^*$ by assuming that the ac-
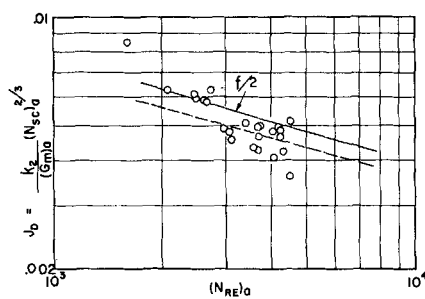

Fig. 2. Binary data: $k_2 = \dfrac{\overline{N_2}(y_3)_{ma}}{(\Delta y_2)_m}$; 2 = benzene, 3 = nitrogen.

tivity coefficients are independent of temperature, and the gas was treated as ideal. The viscosity of the gas mixture was estimated by the method of Wilke (7) using experimental values (8) for the viscosities of the pure components. The viscosity and density were evaluated at the bulk gas composition and temperature. Sources of other physical properties are given elsewhere (8).

RESULTS

A number of preliminary binary runs were made in which pure benzene was vaporized into nitrogen. Gas Reynolds numbers were varied from 940 to 4,500 and liquid Reynolds numbers from 430 to 990. Runs were made with and without benzene in the entering gas and with both small and large rates of vaporization and liquid temperature changes. The decrease in liquid temperature from inlet to outlet varied from 2.4° to 10.2°C. The results are in reasonable agreement with earlier work when the usual log-mean driving force calculated on the basis of terminal compositions and temperatures is used (1).

In Figure 2 the binary results are compared with the Chilton-Colburn equation [the binary form of Equations (10) and (19)]. The *f*/2 line is the same value used in the ternary calculations, and the binary data are seen to be somewhat lower than this line. There was no apparent correlation between the measured mass transfer coefficient and the change in liquid temperature through the column.

TABLE 1. TYPICAL VALUES OF D_{ij}, SQ. FT./HR.

35°C., 1 atm.

Acetone = 1	Benzene = 2
Nitrogen = 3	Helium = 3

$D_{13} = 0.397$	$D_{13} = 1.59$
$D_{23} = 0.346$	$D_{23} = 1.50$
$D_{12} = 0.146$	

Fifteen ternary runs were made at average gas Reynolds numbers in the range of 2,400 to 5,500 with most in the range of 3,000 to 4,000. The liquid Reynolds numbers were in the range of 435 to 1,030 with most around 500. Nine of the runs used helium and six used nitrogen. The entering gas had acetone mole per cents varying from 0 to 15.9, and the exit gas had benzene mole per cents from 2.5 to 5.6. The inlet liquid composition was varied from pure benzene to 17.9 mole % acetone in benzene. The inlet temperatures varied from 29° to 42°C. and the column pressure from 764 to 907 mm. Hg. The composition and temperature variations were carried out in order to cover regions of both strong and weak interactions. The decrease of liquid temperature from inlet to outlet varied from 2.3° to 12°C.

Table 2 shows some of the experimental and computed values for typical ternary runs. Species 1 is acetone and 2 is benzene. It is seen that the predictions of the film equations are closer to experiment than those of the Prandtl-Taylor equations. Although this was usually the case, the differences are not large enough to be significant.

All the experimental fluxes which are presented were obtained from the gas measurements. In general an independent determination of the fluxes from the liquid measurements was not possible (8), but in runs T1 to T8 the acetone fluxes could be determined from the liquid measurements essentially independently of the gas measurements. For these cases the average deviation between the two methods was 19%, exclusive of one run where the acetone flux was very small and the deviation was 68%. This check is considered to be quite satisfactory, considering the small fluxes which are included and the very large interactions which are being sought.

The use of the acetone fluxes determined from the liquid measurements in place of those determined from the gas measurements would have negligible effect on the conclusions of this study.

The predictions of the ternary Chilton-Colburn model were found to be consistently inferior to those of the other two, and this fact, combined with the basic inconsistency of the model, led to its rejection from further consideration. Thus of the interacting equations only the Prandtl-Taylor and film equations are considered, and since they give almost the same results in this work, they can be jointly referred to as the *interacting equations*, as opposed to Equation (19), the noninteracting equation.
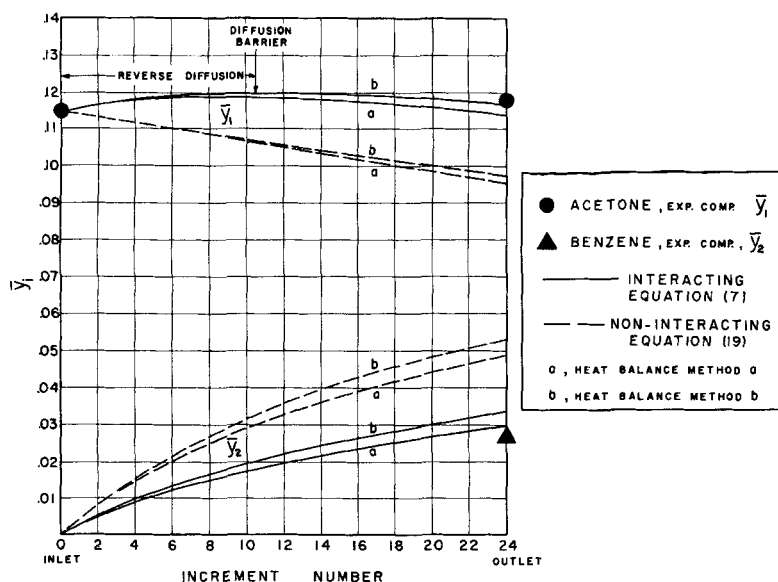
Fig. 3. Computed and measured compositions, run T 14, helium carrier.

Figure 3 shows measured terminal gas compositions (mole fractions of acetone and benzene) for a representative run and gas compositions throughout the column, computed from the interacting and noninteracting equations, Equations (7) and (19) respectively. Position down the column is measured in terms of the increments used in the computations, and the increment number refers to the end of the increment. The curves shown were computed from the film model, but the Prandtl-Taylor predictions on this scale graph are barely distinguishable from those shown.

The figure also contains the results obtained with the two different types of heat balances, and it is seen that the concentration profiles by the two methods do not differ significantly, indicating that the fluxes are not strongly temperature dependent. This was true in all the runs. The computed temperature profiles down the column were usually about the same with both the interacting and noninteracting rate equations. As mentioned in runs T1 to T5 (all nitrogen runs) only heat balance method a was used; all the other computations which are presented were carried out with heat balance method b. The computed liquid temperature at the 24 increment by method b averaged 1.6°C. lower than the measured values. An exact match was not demanded because of the relative insensitivity of the fluxes to liquid temperature and because of the desire to have the best match occur when the computed mean total flux equaled the measured value.

Figure 4 compares the mean acetone and benzene fluxes computed by the noninteracting equations with the measured values for all the ternary

runs, and in Figure 5 the values computed by the interacting equations are compared with the same data. Again these later values are from the film model, but the Prandtl-Taylor values are, as before, about the same as those shown.

DISCUSSION

The method of comparing theory and experiment raises some points which bear preliminary discussion. If Equation (7) and all the associated computations are exact, then the 24 increment in Figure 3 corresponds to the exit of the column and the computed curves give the correct gas composition at any position down the column, as well as at the exit. If the equation, after integration, does not exactly predict the measured exit compositions, then it is convenient in analyzing the results to have a method of comparing the rate equations to experiment without having to rerun the entire program. Examination of Equation (21) shows that the coefficient and interfacial area appear as a product, $k_i \Delta A$, so with concurrent flow a decrease in the area of an increment is equivalent to holding the increment area constant and decreasing both mass transfer coefficients over the increment by the same factor. Therefore any computed concentration profile from the inlet to the j increment is identical to the profile which would be obtained for the entire column if both mass transfer coefficients at every point had been taken as $j/24$ times the values actually used.

Consequently by a material balance the computed mean fluxes at the j increment (these means are necessarily defined as the computed rate of transfer from the inlet to the j incre-
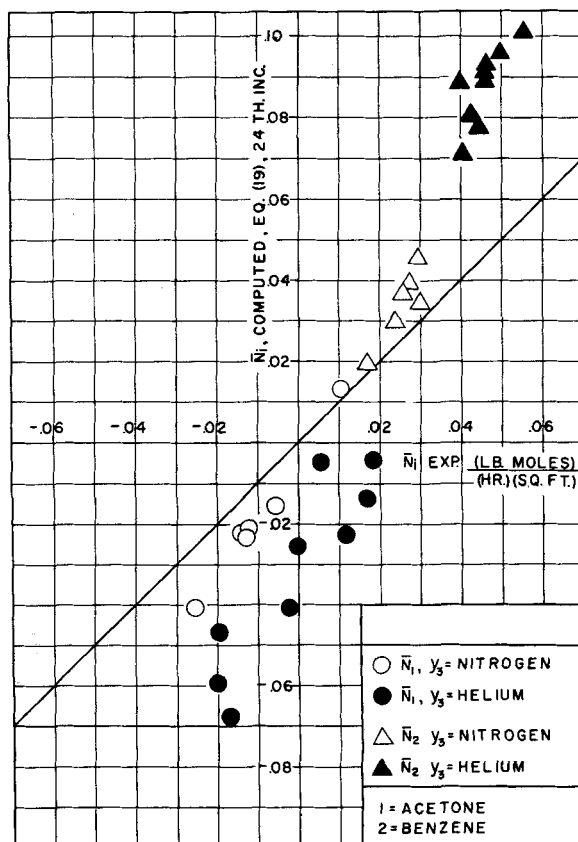

Fig. 4. Comparison of noninteracting equation with experiment.

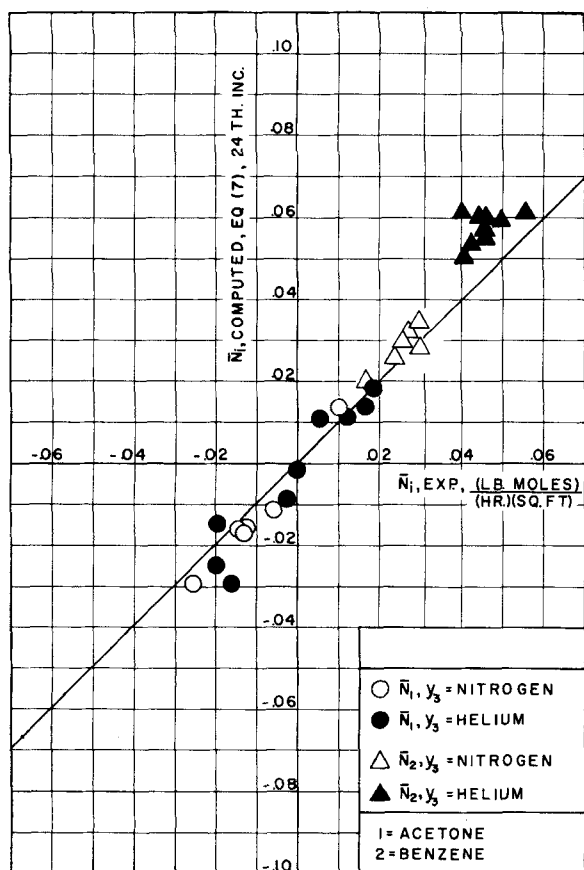Fig. 5. Comparison of interacting equation with experiment, 24 increment.

Fig. 6. Comparison of interacting equation with experiment, 22 increment.

ment per unit interfacial area of the entire column) equal the mean fluxes which would be obtained at the 24 increment (the column exit) if both mass transfer coefficients were $j/24$ times the values actually used in the computations.

The above discussion needs one qualification. If the column exit is to be considered at the j increment, then the liquid-temperature profile from the inlet to the j increment must correspond to the profile in the column. Heat balance method b approximately satisfies this criterion since it is designed to give, on the average, the measured exit liquid temperature when the computed mean total flux has the correct value; this occurs, by definition, at the j increment. Conversely the computed liquid temperature at the 24 increment does not equal the measured exit value if the computed mean total flux up to this point does not equal the experimental value.

Noninteracting Equations

The measured exit compositions followed fairly closely the predictions of the interacting equations as the interactions increased, while the predictions of the noninteracting equations become progressively poorer indicating that the interactions predicted by theory did occur.

The predictions of the noninteracting equations are compared with experiment for all ternary runs in Figure 4. (The 45-deg. line corresponds to a perfect correlation.) The predictions are extremely poor, and in all runs the deviation between calculated and measured fluxes increased as the interactions increased. The four points in the lower right-hand quadrant correspond to runs in which the computed direction of transfer (the net value over the column) was opposite to the measured direction.

Although a significant quantitative measure of the deviation between the computations and experiment does not appear to be possible, the average deviation of 134% (neglecting the one run in which the experimental acetone flux was practically zero) is a somewhat useful figure for later comparisons.

The extremely wide deviations between the predictions of the noninteracting equations and experiment cannot be caused by a liquid or interfacial resistance (reverse diffusion for example cannot be caused by resistances of this type), by incorrect liquid temperatures (any change in liquid temperature will improve the correlation for one component and make it worse for the other), or by any other
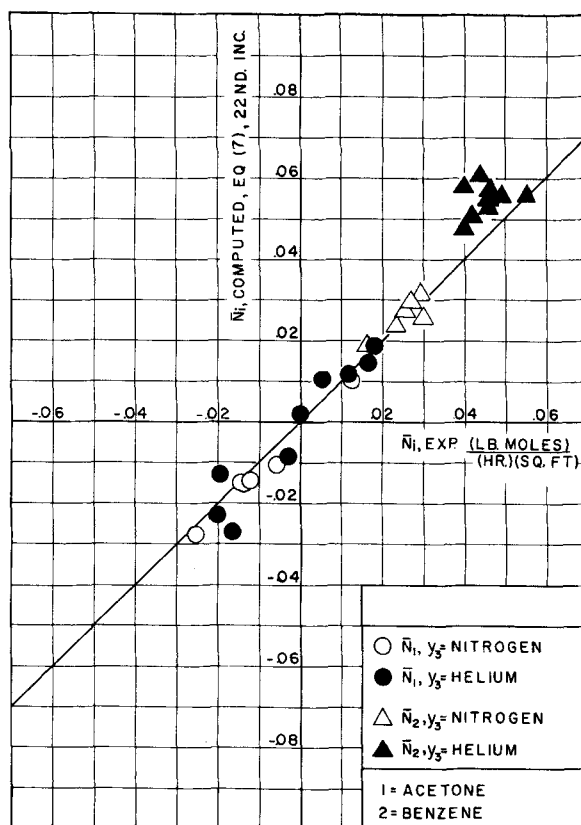
reasonable error in computation or measurement. Although these effects can all be ruled out on individual grounds, the simplest argument lies in the fact that by far the major part of the deviation between the noninteracting equations and the measurements is predicted by the interacting theory.

Interacting Equations

In every run but one the predictions of the interacting equations were significantly closer to experiment than those of the noninteracting equations, implying that in all but one run the actual effect of the interactions was considerably greater than the experimental errors and errors in the computations. This is seen in the representative runs in Table (2) and Figure 3 and in Figure 5 where the computed mean fluxes up to the 24 increment for all the ternary runs are compared with experiment. Comparison of this latter figure with Figure 4 shows the marked improvement in correlation obtained by including the interaction effects. The average deviation is 36%, almost a fourfold improvement over the noninteracting equations.

In one run there were negligible interactions (the system was dilute), and in this run both the interacting and noninteracting equations made about the same predictions which were in reasonable accord with experiment.

TABLE 2. TYPICAL MEASURED AND COMPUTED VALUES AT 24 INCREMENT

Run T3
Nitrogen carrier, heat balance a
Inlet liquid = 35°C.

	$\overline{N_1}$	$\overline{N_2}$	$(\overline{N_1} + \overline{N_2})$	Exit liq. temp., °C.
Experimental	—0.0145	0.0298	0.0153	31.4
Noninteracting	—0.0221	0.0343	0.0122	31.3
Film	—0.0159	0.0285	0.0126	31.8
Prandtl-Taylor	—0.0161	0.0280	0.0119	31.5

Run T6
Helium carrier, heat balance b
Inlet liquid = 34.6°C.

	$\overline{N_1}$	$\overline{N_2}$	$(\overline{N_1} + \overline{N_2})$	Exit liq. temp., °C.
Experimental	—0.0200	0.0495	0.0295	28.2
Noninteracting	—0.0593	0.0958	0.0365	26.8
Film	—0.0249	0.0596	0.0347	27.6
Prandtl-Taylor	—0.0283	0.0633	0.0350	27.6

Run T14
Helium carrier, heat balance b
Inlet liquid = 41.2°C.

	$\overline{N_1}$	$\overline{N_2}$	$(\overline{N_1} + \overline{N_2})$	Exit liq. temp., °C.
Experimental	0.0188	0.0459	0.0577	29.6
Noninteracting	—0.0225	0.0913	0.0688	28.5
Film	0.0114	0.0579	0.0693	28.1
Prandtl-Taylor	0.0076	0.0618	0.0694	28.0

The values shown were obtained from the film model. Although the Prandtl-Taylor model gave essentially the same results, the deviations, as mentioned, were in general slightly greater than the deviations of the film model. The average deviation of the Prandtl-Taylor model was 45% at the 24 increment.

There are further points to be observed in comparing Figures 4 and 5. The four points in the lower right quadrant of Figure 4 are shifted to the upper right quadrant of Figure 5 showing that the quite significant net reverse diffusion over the column was predicted by the interacting equations.

In these runs the calculations indicate that in the upper portion of the column acetone vaporized in the direction opposite to its concentration gradient (reverse diffusion). Further down the column the drop in liquid temperature shifted the vapor pressures, and gas compositions changed as well. Therefore acetone condensed, though at a much lower rate than would be predicted by the noninteracting equations for these conditions. A region in which calculations indicate that reverse diffusion existed is shown in Figure 3. (If the liquid temperature had been held constant, a considerably larger net reverse diffusion would have taken place.)

It should be pointed out that the reverse diffusion which occurred in these experiments cannot be simply interpreted as a convective effect caused by the vaporization of the benzene, for the effective diffusion coefficient of acetone is frequently negative in these reverse diffusion regions. This means that the acetone diffusion flux (the flux with respect to the mean molar velocity) as well as the convective flux is in the direction of increasing acetone concentration.

In general the interactions in the helium runs were greater than in the nitrogen runs, not only because the diffusivity ratio r is much greater in the former than in the latter case but also because the temperature and composition in the helium runs were such that they tended to emphasize the interactions. Although the noninteracting equations essentially ignore the differences between helium and acetone, the interacting equations account for the differences by an increase in the value of δ. Consequently, as shown by a comparison of Figures 4 and 5 and as demanded by experiment, the interaction terms apply a much larger correction to the helium runs than to the nitrogen runs.

A closer examination of Figure 5 shows that the corrections are not quite great enough, for the acetone

points are generally below the 45-deg. line and the benzene points above the line. Also the points with helium are further off than those with nitrogen.

Consequently, even though the results demonstrate that the interaction phenomena not only exist but are described comparatively well by the theory developed in Part I, some refinements of the analysis are desirable. These refinements are necessarily of a second order and would have negligible effect on the gross errors of the noninteracting equations.

Use of Measured Binary Coefficient

The interacting theory can be considered to be based on binary mass transfer data in the sense that the theory predicts the deviations between the mass transfer in a given ternary system and the transfer which would take place in a binary system operating with the same hydrodynamics as the ternary system. This viewpoint was used explicitly in deriving the film model and is implicit in the Prandtl-Taylor model. In the actual ternary calculations the calibrating binary coefficient used was the value given by the $f/2$ line in Figure 2. This was obtained with nitrogen as the inert gas. Although the binary data obtained in this work do not differ significantly from the $f/2$ line, the best fit with the same slope (the line is approximately linear over the range of interest) is 9.6% lower than $f/2$ line. Hence if the binary runs made in this work are used to calibrate the ternary runs, the ternary coefficients which were used should be decreased by 9.6%, which means that the computations at about the 22 increment rather than the 24 increment should have been compared with the experimental values. If this is done, the correlation shown in Figure 6 results. The average deviation is now 29%. Although this correlation might be accepted as a measure of the accuracy of the interacting theory, a deeper insight into the results as well as a check of the internal consistency of the theory may be obtained by considering the behavior of the total flux.

The mean total flux at the 22 increment is compared with experiment in Figure 7. This same graph applies to both the interacting and noninteracting calculations. The computed nitrogen values are close to experiment, while the helium values are generally high. The computed liquid temperatures at this increment average 0.4°C. above the corresponding measured values in the nitrogen runs and 1.3°C. below the measured values in the helium runs. The liquid temperatures in the helium runs are low because the

total fluxes at this increment are greater than experiment.

In every run the mean total flux predicted by the interacting equations was almost the same as that predicted by the noninteracting equations at every point in the column (see examples for the 24 increment in Table 2); the theoretical interactions only altered the individual acetone and benzene fluxes. This indicates that not only is D_{12} close enough to D_{13} to allow Equation (20) to hold but also that the total flux is not sensitive to the individual acetone and benzene compositions in the vapor and liquid.

Therefore the computed mean total flux does not depend to any significant extent upon the interaction theory; any theory which is consistent in the sense used in Part I, and which does not predict wildly incorrect individual fluxes, will give practically the same mean total flux in this work.

Furthermore since Equation (20) holds, the position at which the computed mean total fluxes best fit the experimental values gives the best calibrating mass transfer coefficient for the ternary runs from the ternary runs themselves, and this coefficient is quite independent of the interactions. (It is tacitly assumed that the present interaction theories are not incorrect in predicting that the total flux closely approximates the normal binary equation when, as in this system, $D_{13}/D_{23} \cong$ 1.1. This seems to be a safe assumption, since it was shown in Part I that the interacting theories are exact in the limit of $D_{13} = D_{23}$.)

Since the total flux in the ternary runs behaves much like the benzene flux in the binary runs, an alternate method of computing the mass transfer coefficients from the ternary data is to treat the pseudo-pure component benzene plus acetone in exactly the same manner as the benzene was treated in the binary runs, that is assume that the correct mean total driving force to use in the integrated form of Equation (20) is the log mean and then use the measured compositions, flow rates, and temperatures to directly compute the calibrating mass transfer coefficient for each run. This method, although less exact than finding the best fit from the machine computations, gives over-all results which are about the same and allows the coefficients for each run to be obtained simply and in a form directly comparable to the binary data.

The values of j_D' so obtained are plotted against average Reynolds numbers in Figure 8. The j_D' fall into two distinct groups, one corresponding to the nitrogen runs and one to the
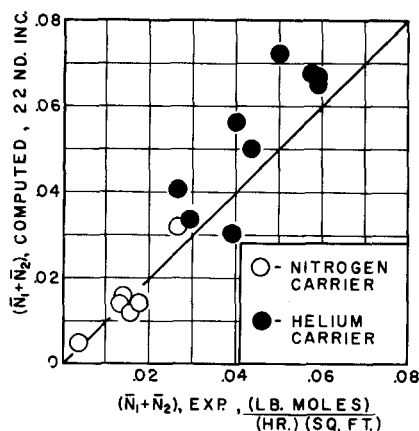

Fig. 7. Comparison of computed and measured mean total fluxes.

helium runs, as would be expected from Figure 7. Not surprisingly, the scatter within each group is greater than in the binary runs.

The best line for the nitrogen runs is within 3% of the value obtained from the binary data. Since the computed individual fluxes in the nitrogen runs check experiment well with coefficients based on this binary coefficient (Figure 6), the results of the nitrogen runs are self-consistent.

The best line for the helium runs however is equal to 0.6 $f/2$, 33% lower than the binary value. If the above number is accepted as a true lowering of the mass transfer coefficient when helium is the stagnant gas, then in the helium runs the computed individual fluxes at the 14 increment should be compared with experiment. If this is done the correlation is improved, but there is no reason to expect this coefficient to be low. There is in fact evidence that the lowering of the coefficient is spurious.

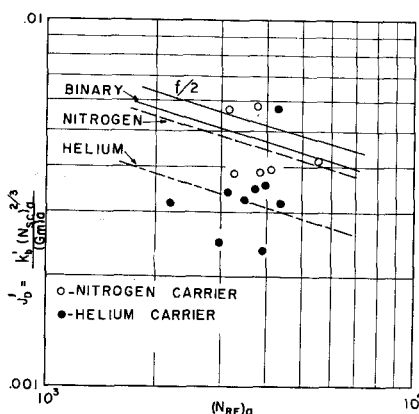The explanation for the apparently low coefficient seems to lie in the fact

Fig. 8. Mass transfer coefficient for total flux

in ternary runs, $k'_b = \dfrac{(\overline{N_1} + \overline{N_2})\, (y_3)_{ma}}{(-\Delta y_3)_m}$.

that the total flux in the ternary runs is more sensitive to liquid temperature than is the benzene flux in the binary runs. (Sensitivity is relative. Acetone in the helium runs is more sensitive than the total flux, but the authors are interested in almost order of magnitude effects with the acetone flux, while with the total flux they are interested in small effects.) This sensitivity occurs because the total driving force in the ternary runs $(\overline{y_3} - y_3^*)$ [Equation (20)] gets small at the column exit.

Even though the sensitivity exits in both the nitrogen and helium runs, the total flux, and corresponding fall in liquid temperature, is higher in the helium runs than in the nitrogen runs. (The one high total flux nitrogen run behaved like the helium runs.) The interfacial liquid temperature must always be lower than the bulk temperature, and this error would be largest in the high total flux runs. It would take on the average only about 2°C. lowering of the interfacial temperature over the column (the actual value varies with the total flux) to bring the helium coefficients up to the binary values, and an effect of this magnitude is not impossible.[*]

Although temperature errors of the same magnitude would occur in the high flux binary runs, the relatively large driving forces in the latter runs are much less temperature sensitive, so a 2°C. lowering of the interfacial temperature would not have been (and was not) visible in the binary runs.

If this explanation is valid, then the interacting theory should be tested by comparing computed and measured individual fluxes at the 22 increment with exit liquid temperatures in the helium runs about 2°C. lower than experiment.

This calculation was carried out in a rough fashion by using the results obtained with heat balance a which gives temperatures which are low by about the above amount.

The result of the calculation leaves Figure 6 essentially the same, except that the high benzene points in the helium runs are moved closer to the 45-deg-line and the acetone points drop slightly below. The average deviation is 33%, hardly changed.

Thus the individual fluxes in the helium runs are predicted reasonably well whether the low helium coefficients are real or are caused by a low interfacial temperature. Moreover whatever the cause of the low helium

coefficients the discrepancies in the results must be considered insignificant when compared with the success obtained with the interacting theory. Since these discrepancies may be attributed to experimental and computational errors, it appears that the interacting theory predicts the individual fluxes within the accuracy of the experiments.

CONCLUSIONS

The present experiments show rather conclusively that ternary mass transfer is indeed described by an equation of the form of (1). In addition the individual fluxes are predicted by the interacting theory within the accuracy of the experiments.

Even though the predictions of the film model are generally closer to experiment than the predictions of the Prandtl-Taylor model, the experiments do not really allow a choice between the two models because of the small differences between them. This arises because at the low Reynolds numbers studied the film resistance predominates over the core resistance in the Prandtl-Taylor model. At very high Reynolds numbers the Prandtl-Taylor equation approaches the multicomponent Reynolds analogy, Equation (22), Part I, and this latter equation differs markedly from the film model in a system of the type studied here. Although generalizations in this case are hazardous because of the many parameters involved, it appears that it may be frequently possible to go to quite high Reynolds numbers before the film and Prandtl-Taylor models diverge markedly. Thus it is quite possible that the comparatively simple film model will have a wide range of applicability even though the Prandtl-Taylor or more refined models may be needed at very high Reynolds numbers.

The advantages of the film model lie not only in its relative simplicity but also in the ease with which it may be extended to more complicated systems such as packed and tray columns. This ease of course should not obscure the fact that the success of a model in a wetted-wall column does not ensure its success in systems where different hydrodynamic conditions prevail. Nevertheless since molecular diffusion plays a significant part in interphase mass transfer, whatever the means of contact, interaction phenomena of the type studied here must exist. Therefore the film model will at least be qualitatively correct, and it is not unreasonable to expect the model to be quantitatively correct as well.

The results demonstrate rather vividly that the gas adjacent to the liquid interface behaves like a laminar film, for if the gas were fully turbulent up to the interface, Equation (22), Part I, would apply and would give much smaller interactions. This does not prove that there is a laminar film in the classical sense, for even in systems with smooth walls the film is more likely to be continuously breaking and reforming. However it has been shown (13) that at the low Schmidt numbers of gases such a region of disturbed fluid will behave as if it were a film because of the relatively short time needed for steady state diffusion to be set up in a fluid element.

Since the ternary system studied here is closely related to the general multicomponent gas, the success of the effective film and Prandtl-Taylor models in this work implies that similar (but not identical) models will be valid, not only in other types of ternary systems, such as ternary equimolal countercurrent transfer (for which the equations were developed in Part I), but also in all the multicomponent systems in which the Maxwell-Stefan equations are valid. The Prandtl-Taylor model can be carried over directly to the general case for example by using the exact or Wilke's approximate solution (17) [Equation (14), Part I] to the Maxwell-Stefan equations for diffusion through the film for any particular determinancy conditions and generalization of Equations (21) and (22), Part I, for the turbulent core (15).

The effective film model would be simpler, but an unambiguous generalization is not possible at this time.

The present recommended design equation for ternary mass transfer are Equations (16) and (17), Part I, with the mass transfer coefficients equal to the coefficients which would be obtained for binary systems in the same equipment with the same hydrodynamics as the ternary system:

$$N_i = k_i \phi_j (\delta_j y_{ij} - y_i) \quad (22)$$

where j becomes S for transfer with one gas stagnant and e for equimolal countercurrent transfer. At very high Reynolds numbers it would be wise to check these film equations with those based on the Prandtl-Taylor model.

An application of the above equation, with a somewhat different type of mass transfer coefficient, to the prediction of plate efficiencies in ternary distillation has already been carried out (13).

ACKNOWLEDGMENT

The authors are grateful for the fellowship assistance to R. T. Sebulsky of

NOTATION

A	=	interfacial area, sq. ft.
j_D	=	j factor
j_D'	=	j factor for total flux
k_L	=	liquid side mass transfer coefficient, ft./hr.
k_b'	=	mass transfer coefficient for total flux, ft./hr.
K	=	over-all mass transfer coefficient, ft./hr.
m	=	vapor-liquid equilibrium constant
n	=	flow rate, lb. moles/hr.
x	=	liquid mole fraction
ϕ,δ,ψ	=	interaction terms as defined by Equations (8), (9), (11), (12), and (15)

Subscripts

a	=	arithmetic average of value at top and bottom of column
j	=	e if equimolal, S if one gas stagnant

Superscripts

*	=	equilibrium value

LITERATURE CITED

1. Canjar, L. N., and T. E. Lonergan, A.I.Ch.E. Journal, 2, 280 (1956).
2. Cairns, R. C., and G. H. Roper, Chem. Eng. Sci., 3, 97 (1954).
3. Emmert, R. E., and R. L. Pigford, Chem. Eng. Progr., 50, 87 (1954).
4. Gilliland, E. R., and T. K. Sherwood, Ind. Eng. Chem., 26, 516 (1934).
5. Johnstone, H. F., and R. L. Pigford, Trans. Am. Inst. Chem. Engrs., 38, 25 (1942).
6. Koo, E. C., Sc.D. thesis, Massachusetts Institute of Technology, Cambridge, Massachusetts (1930).
7. Reid, R. C., and T. K. Sherwood, "The Properties of Gases and Liquids," McGraw-Hill, New York (1958).
8. Sebulsky, R. T., Ph.D. thesis, Carnegie Institute of Technology, Pittsburgh, Pennsylvania (1961).
9. Sherwood, T. K., and R. L. Pigford, "Absorption and Extraction," McGraw-Hill, New York (1952).
10. Shulman, H. L., and L. J. Delaney, A.I.Ch.E. Journal, 5, 290 (1959).
11. Tierney, J. W., L. F. Stutzman, and R. L. Daileader, Ind. Eng. Chem., 46, 1595 (1954).
12. Toor, H. L., A.I.Ch.E. Journal, 3, 198 (1957).
13. ———, and J. M. Marchello, ibid., 4, 97 (1958).
14. Toor, H. L., and J. K. Burchard, ibid., 6, 202 (1960).
15. Toor, H. L., ibid., p. 525 (1960).
16. Westkaemper, L. E., and R. R. White, ibid., 3, 59 (1957).
17. Wilke, C. R., Chem. Eng. Progr., 46, 95 (1950).